ELSEVIER

Journal of Nuclear Materials 313–316 (2003) 748–753

journal of nuclear materials

www.elsevier.com/locate/jnucmat

Measurements of hydrogen negative ion and its comparison with the molecular hydrogen spectra in divertor simulator MAP-II

S. Kajita [a,*], S. Kado [b], N. Uchida [a], T. Shikama [a], S. Tanaka [a]

[a] *Department of Quantum Engineering and Systems Science, School of Engineering, The University of Tokyo, 7-3-1 Hongo, Bunkyo-ku, Tokyo 113-8656, Japan*

[b] *High Temperature Plasma Center, The University of Tokyo, Tokyo, Japan*

Abstract

Negative ion density and vibrationally excited molecular hydrogen were compared in divertor simulator MAP-II. Laser photo-detachment technique was used for the negative ion measurement, and Fulcher-α band ($d^3\Pi_u \rightarrow a^3\Sigma_g^+$) spectra were used to determine the vibrational distribution of excited hydrogen molecules in the electronic ground state. As the hydrogen gas pressure increased, the negative ion density increased at first, then started to decrease as the hydrogen pressure exceeded 10 mTorr. On the other hand, the vibrational temperature measured in the same condition decreased when the hydrogen gas pressure became higher than 10 mTorr. We found that the decrease in the vibrational temperature resulted in the decrease in the negative ion density.

PACS: 52.40.H

Keywords: Divertor; Plasma detachment; MAR (molecular activated/assisted recombination); Vibrational excitation; Negative ion; Laser photodetachment technique

1. Introduction

High heat flux evolves critical problems in divertor regions such as plate erosion. Recently, forming a detached plasma has been considered as one of the methods to reduce the heat flux to the wall. Some observations of detached divertor plasmas strongly indicate that the plasma detachment is closely related to the volume recombination of divertor plasmas [1,2]. The following four processes [3,4] are included in the theoretical analysis of divertor plasma recombination,

$$H^+ + e^- \rightarrow H(n) + h\nu, \tag{1}$$

$$H^+ + e^- + e^- \rightarrow H(n) + e^-, \tag{2}$$

$$H_2(v) + e^- \rightarrow H^- + H, \quad \Rightarrow H^- + H^+ \rightarrow H + H(n) \quad n = 2 \text{ or } 3, \tag{3}$$

$$H_2(v) + H^+ \rightarrow H_2^+ + H, \quad \Rightarrow H_2^+ + e^- \rightarrow H + H(n) \quad n \geqslant 2. \tag{4}$$

Process (1) is the radiative recombination and (2) the three body recombination. Processes (3) and (4) are the processes called molecular activated/assisted recombination (MAR) in which the vibrationally excited hydrogen molecules play an important role. In the process (3), negative hydrogen ions are generated by dissociative electron attachment to the hydrogen molecules, and the plasmas are extinguished through a mutual neutralization process. Therefore, it is important to measure negative ion density and vibrationally excited hydrogen

* Corresponding author. Tel.: +81-3 5841 6970; fax: +81-3 3818 3455.

E-mail address: s_kajita@flanker.q.t.u-tokyo.ac.jp (S. Kajita).

0022-3115/03/$ - see front matter
PII: S0022-3115(02)01417-4

molecules in order to examine experimentally if the process (3) can be identified in the divertor region.

For plasmas in negative ion sources, there are some publications on the experimental comparison between the measured negative ion density and the vibrational population. In these studies, negative ion density was measured using laser photo-detachment technique [5]. On the other hand, vibrational populations were measured using coherent anti-Stokes Raman scattering (CARS) [6] or vacuum-ultraviolet (VUV)-laser-induced fluorescence (LIF) [7].

However, since the port access is limited in the divertor plasmas, passive spectroscopic measurement is rather easy to be applied. Moreover, if one observes visible light, fiber optics can be used. In this point of view, Fulcher band visible spectroscopy [8] ($d^3\Pi_u \rightarrow a^3\Sigma_g^+$) is applied to the divertor plasmas [9,10]. The objective of the present paper is to find the relationship between H^- and $H_2(v)$ experimentally in the divertor simulator MAP-II, using the photo-detachment technique for the former and the Fulcher bands emission spectroscopy for the latter, respectively. After a brief description on the experiments in Section 2, the results of negative ion density and vibrational temperature measurements are shown in Section 3. Then, a comparison is made between them in Section 4. Finally, conclusions are given in Section 5.

2. Experiments

Divertor simulator MAP (Material And Plasma)-II is assembled by differentially pumped dual chambers, the source chamber and the target chamber, which are connected by a drift tube. Cylindrical plasma is generated by an arc discharge between LaB_6 cathode and an anode pipe, and confined radially by a magnetic field of about 100 gauss in the target chamber. Typical discharge voltage and current are about 85 V and 45 A, respectively, for the feeding He gas rate into the arc source of about 200 sccm. The additional gas is injected into the target chamber and the pressure is measured using a Baratron pressure gauge in the target chamber.

Fig. 1 shows the schematic view of the experimental setup. Negative ion density was measured in the target

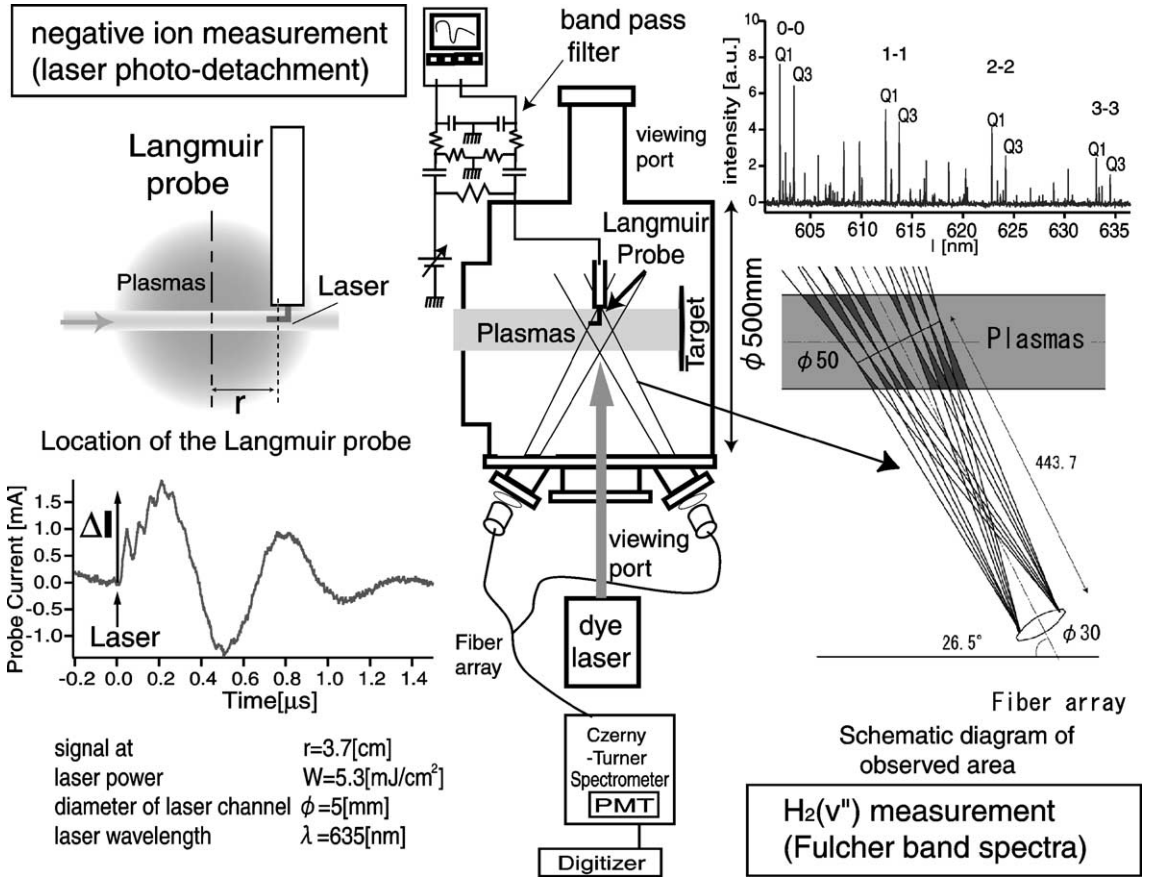

Fig. 1. Experimental arrangement. Negative ion density is measured using Laser photo-detachment. $H_2(v)$ is measured using Fulcher band spectra.

chamber using laser photo-detachment technique combined with a Langmuir probe. A dye laser (ND6000: continuum) excited by a YAG laser ($\lambda = 532$ nm) was used as a photon source with a wavelength of 635 nm. Photo-detachment fraction of H^- ion, δn_-, due to the laser pulse, depends on both laser power and its wavelength, and can be written as $\delta n_-/n_- = 1 - \exp(-W\sigma_{pd}/S_l h\nu)$ [5], where σ_{pd} is the cross-section for photo-detachment, W the laser power and S_l the cross-section of the laser beam. In this paper, a ratio of the photo-detachment fraction to the initial negative ion n_- was chosen around 0.5–0.9, since too high power of the laser leaded to the ablation of the probe surface. Negative ion density can be obtained from the ratio of the photo-detachment signal value ΔI to the electron saturation current I_{es};

$$\frac{\Delta I}{I_{es}} = \frac{\delta n_-}{n_e} = \frac{n_-}{n_e}(1 - \exp(-W\sigma_{pd}/S_l h\nu)), \quad (5)$$

where n_e is the electron density. Due to the electron density fluctuations caused possibly by the plasma instabilities, the probe characteristics in the typical MAP-II hydrogen discharges are highly disturbed. The fluctuation level, $\widetilde{I_{es}}/I_{es}$, is typically 40%. This value indicates that the fluctuation is much larger than the photo-detached electron signals. Fast fourier transform (FFT) analysis of the electron saturation current indicates that the photo-detached signal can be distinguished from the fluctuations, since most of the fluctuation power is in a frequency range lower than several hundreds of kHz, while the frequency of the photo-detachment signal is over 1 MHz. Therefore, the R–C band pass filter was used to remove the fluctuation noises [11].

A 1 m Czerny Turner monochromator with a photomultiplier tube was used for the Fulcher bands spectroscopy. $d^3\Pi_u$ state distribution was obtained by operating the Franck–Condon matrix for the ground states distribution characterized by T_{vib}. The cross-section of the $X^1\Sigma_g^+(v = 0) \rightarrow d^3\Pi_u$ excitation was taken from Ref. [12] and the vibrationally resolved excitation rate coefficients were calculated by reducing the threshold energy according to the energy difference from the $v = 0$. For this calculation, the measured electron temperatures were used. On the other hand, dividing the measured relative band intensities by the branching ratios of the Fulcher band emission, the relative population of the vibrational distribution of the upper Fulcher states can be determined. In the analysis, the vibrational distribution in the electronic ground state was described as Boltzmann distribution with the vibrational temperature T_{vib}. Assuming the Franck–Condon principle in electron impact excitation processes, distribution of the upper Fulcher states can be derived. Comparing this calculation with the spectral intensity for the diagonal Fulcher band, the vibrational population of the electronic ground state can be obtained as the distribution equivalent to the Boltzmann temperature, T_{vib}. Since the electron density in this experiment was low ($\leqslant 5\times10^{11}$ cm^{-3}), the above-mentioned assumption (the coronal model) might be valid. For higher density in divertor plasmas, it is reported that a collisional-radiative model needs to be applied [10]. Note that the only line integral values across the plasma column are available for the moment, which are shown in Fig. 1. The total intensity was estimated as the integral over the rotational quantum numbers, which were deduced from several Q-branch spectra by assuming rotational temperature.

3. Results

Fig. 2 shows the radial profiles of electron density (a), electron temperature (b) and negative ion density (c). As seen in the figure, the profile of the negative ion density has a hollow profile while the electron density and the electron temperature have a peak in the center. Additionally, one can see that the negative ion density profile was strongly related to the electron temperature. Higher negative ion density is due to lower electron temperature.

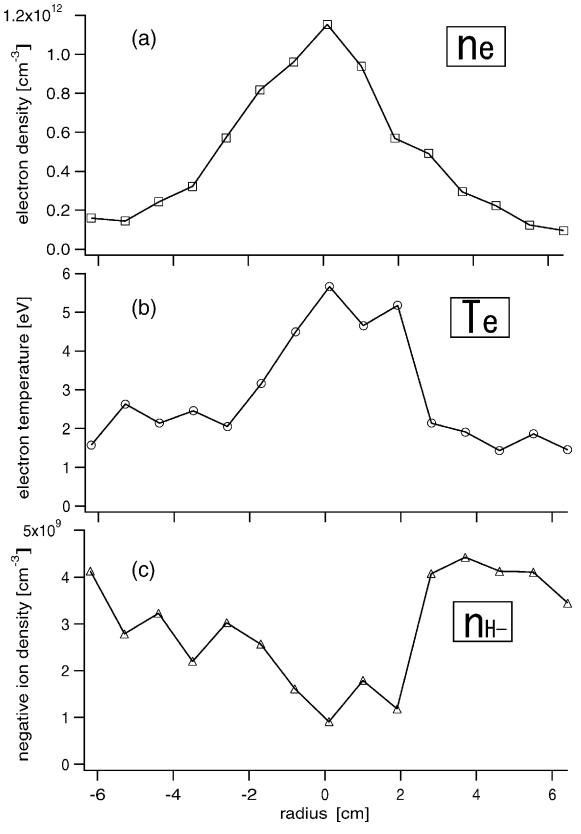

Fig. 2. Radial profile of electron density (a), electron temperature (b) and negative ion density (c) in MAP-II.

The negative ion density was about 1×10^9–4×10^9 cm^{-3} in this condition. Total gas pressure was 12 mTorr and the helium background gas pressure was about 2.7 mTorr.

Fig. 3 shows the measured electron density (a), electron temperature (b) and negative ion density (c) at a radius of 3.7 cm as functions of the gas pressure. The negative ion density increases in the first half of the figure as the hydrogen gas pressure increases, then starts to decrease in the pressure higher than 10 mTorr. It has been confirmed that the width of electron density and temperature profiles at hydrogen gas pressure of around 1 mTorr were almost same as that in 9 mTorr shown in Fig. 2. This suggests the radial diffusion is not much changed by increasing the neutral pressure in this range. If the strong recombination occurs in higher pressure, the profile could change. However, under the conditions in this series of the experiment, the recombination phenomena are not clearly observed. Therefore, taking into consideration the fact that the radial width in which H^- exists is about 4 cm, the profiles of the parameters can be assumed to be constant, and the dependence can be discussed at the fixed radial position, 3.7 cm. Reasons for this phenomenon are discussed in Section 4.

Fig. 4 shows a comparison of measured and calculated relative vibrational population in $d^3\Pi_u$ of H_2. As seen in this Figure, the measured spectra for 3.4 and 12 mTorr can be attributed to the ground state vibrational population around 7000 and 3500 K, respectively.

Fig. 5 shows the dependence of the vibrational temperature on the hydrogen gas pressure. Although the T_{vib} probably does not have the strong H_2 pressure dependence below 5 mTorr, it clearly decreases as the gas pressure increases to above 6 mTorr. Since high energy electrons are needed to produce vibrationally excited hydrogen molecules, a decrease in the electron temperature may have an effect on reducing the vibrational excitation, namely T_{vib}. Note that the obtained rotational temperature were 480–600 K for $v' = v'' = 0$, 370–450 K for $v' = v'' = 1$, 310–370 K for $v' = v'' = 2$ and 250–400 K for $v' = v'' = 3$, respectively.

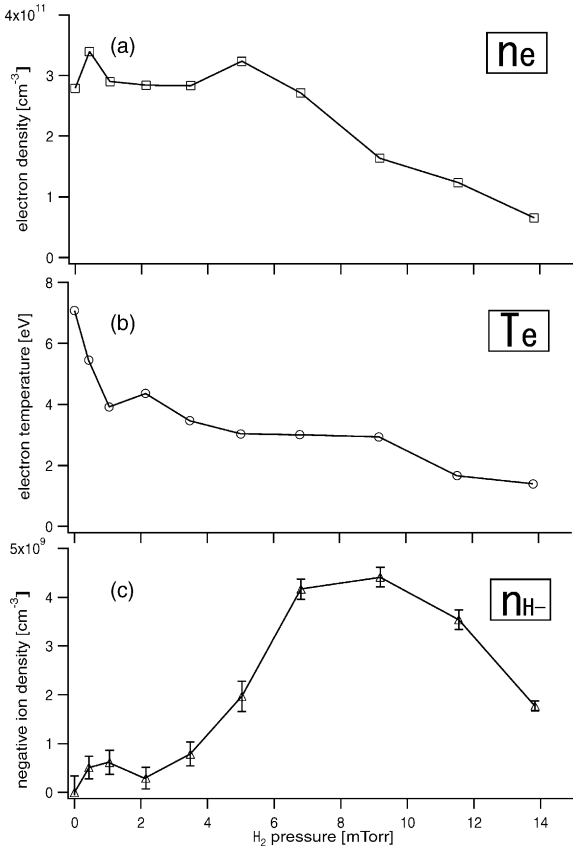

Fig. 3. Measured electron density (a), electron temperature (b) and negative ion density (c) as a function of hydrogen gas pressure. Error in (c) includes only that from the photo-detached signal.

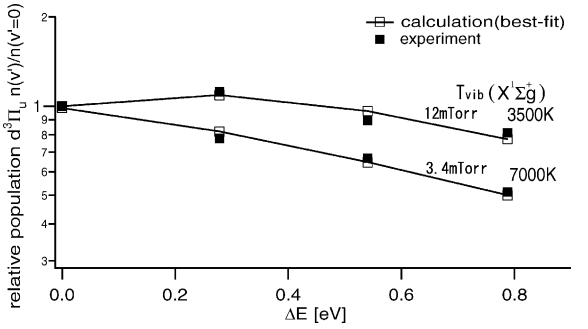

Fig. 4. Comparisons of the measured and the calculated relative vibrational population of the upper state $d^3\Pi_u$ of the hydrogen molecule. Measured spectra for 3.4 and 12 mTorr can be best-fitted to that calculated for the ground state vibrational population around 7000 and 3500 K, respectively.

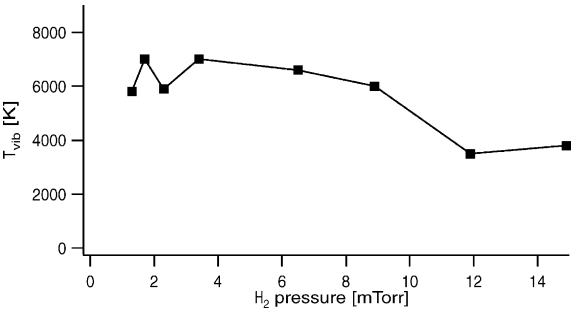

Fig. 5. Measured vibrational temperatures as a function of hydrogen gas pressure.

4. Discussions

The production processes of negative ions are highly dominated by the electron attachment to the vibrationally excited hydrogen molecules, $H_2(v'' \geqslant 4) + e^- \rightarrow H^- + H$. The main negative ion loss mechanisms in our apparatus are (a) mutual neutralization, $H^- + H^+ \rightarrow 2H$, (b) electron collision process, $H^- + e^- \rightarrow H + 2e^-$ and (c) transport loss. The measurements of n_e, T_e and T_{vib} yield the negative ion density according to the following equation,

$$\frac{dn_{H^-}}{dt} = n_e \sum_{v''} n_{H_2(v'')} \alpha_{e,H_2(v'')} - n_{H^-} n_e \alpha_{e,H^-} - n_{H^-} n_{H^+} \alpha_{H^+,H^-} - n_{H^-}/\tau, \quad (6)$$

where $\alpha_{e,H_2(v'')}$ [13], α_{e,H^-} [14] and α_{H^+,H^-} [15] are the rate coefficients of electron attachment, mutual neutralization and electron impact detachment processes, respectively, and τ is the confinement time of negative ions. The value τ was described by an effective transport characteristic length ΔL divided by negative ion velocity v_{H^-}, namely $\tau = \Delta L/v_{H^-}$. It can safely be assumed that the ion sound velocity gives the upper limit of the drift velocity of the negative ions. On the other hand, it can be thought that ΔL is between Δr_- or R and L, where Δr_- the radial width of the H^- density which is close to the radius of the plasma column R and L the plasma length in the target chamber. In this experiments, $\Delta r_- \simeq 4$ cm, $R \simeq 5$ cm and $L \simeq 50$ cm. Therefore, $\Delta r_-/\sqrt{kT_e/M} \leqslant \tau \leqslant L/\sqrt{kT_i/M}$ with $T_e \gg T_i$ in our case.

Fig. 6(a) shows the pressure dependence of the negative ion production rate calculated using the first term of the right-hand side of Eq. (6). In the calculation, we used the electron temperature and density measured with the Langmuir probe at $r = 3.7$ cm, where the negative ion density was measured. Open circles represent the calculated production rate assuming constant T_{vib} (7000 K), while squares represent that from experimentally derived T_{vib}. This result implies that the decrease of T_{vib} above 10 mTorr, typically from 7000 to 4000 K, led to the reduction of the production rate to lower than 1/10 of magnitude. Fig. 6(b) is the calculated extinction rate obtained from the sum of the last three terms of the right-hand side of Eq. (6) divided by n_{H^-}. Open squares and circles represent the calculated negative ion density using R and L for ΔL, respectively. In Fig. 6(c), open squares represent the calculated n_{H^-} in which experimentally obtained T_{vib} and $\Delta L = R$ ($= 5$ cm) are used, while full triangles represent the measured n_{H^-}. Each error bars of open squares represent the sensitivity of the H^- density calculations obtained by varying each value by $\pm 10\%$. This figure indicates the existence of radial loss in negative ions. If we use $\Delta L = L$ in the calculations, the results become larger by a factor of three. In the same manner, if T_{vib} is a constant value 7000 K, the calculated results cannot reproduce the steep decay of the experimental n_{H^-} in the range higher than 10 mTorr. Although the value of both ΔL and drift velocity can be changed at the same time, ion sound velocity may be an upper limit and R or possibly Δr_- be a lower limit of the free parameters. More quantitative investigation is of a future work.

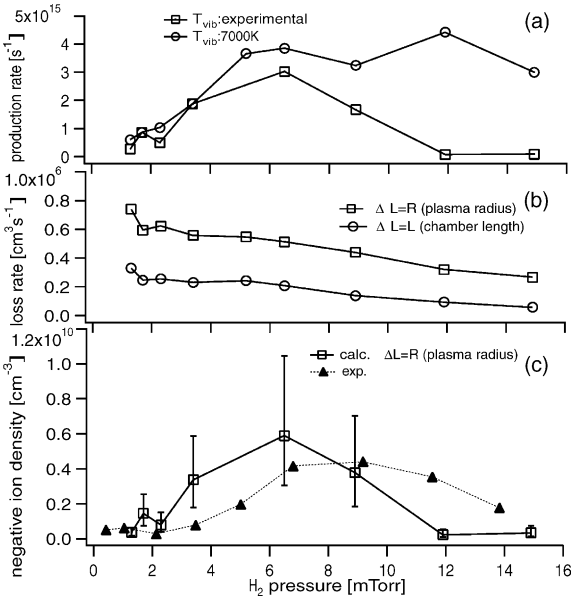

Fig. 6. (a) and (b) are the production and loss rate of negative ions, respectively. (c) is the negative ion density, where full triangles represent the measured H^- density and open squares represent the calculated H^- density using R as a effective transport characteristic length. Each error bars of open squares represent the sensitivity of the H^- density calculations obtained by varying each measured parameter by $\pm 10\%$.

5. Conclusions

Negative ion density was measured in the Divertor simulator MAP-II over a hydrogen gas pressure from several mTorr to 15 mTorr. Negative ion density increased as the gas pressure increased, then started to decrease when the gas pressure exceeded 10 mTorr. Obtained vibrational temperature of hydrogen molecules in the ground-states were 6000–7000 K at the hydrogen gas pressure lower than 10 mTorr, and then decreased to around 4000 K when the pressure exceeded 10 mTorr. The production rate and loss rate of negative ion density were evaluated from experimentally obtained parameters, then negative ion density were derived from balancing these two rates. The results indicate that the decrease of T_{vib} led to the drop of negative ion density in our condition.

More detailed quantitative analysis based on more precise measurements of both H^- and $H_2(v)$ are planned together with the ion flux measurement for a sufficient identification of the dominant recombination processes occurring in the divertor region.

References

[1] D. Lumma, J.L. Terry, B. Lipschultz, et al., Phys. Plasmas 4 (1997) 2555.
[2] N. Ohno, N. Ezumi, S. Takamura, et al., Phys. Rev. Lett. 81 (1998) 818.
[3] R.K. Janev, D.E. Post, W.D. Langer, et al., J. Nucl. Mater. 121 (1984) 10.
[4] S.I. Krasheninnikov, A.Yu. Pigarov, D.A. Knoll, et al., Phys. Plasmas 4 (1997) 1638.
[5] M. Bacal, G.W. Hamilton, Phys. Rev. Lett. 42 (1979) 1538.
[6] M. Pealat, J.-P.E. Taran, M. Bacal, F. Hillion, J. Chem. Phys. 82 (1985) 4943.
[7] T. Mosbach, H.-M. Katsch, H.F. Dobele, Phys. Rev. Lett. 85 (2000) 3420.
[8] U. Fantz, B. Heger, Plasma Phys. Control. Fusion 40 (1998) 2023.
[9] U. Fantz et al., J. Nucl. Mater. 266–269 (1999) 490.
[10] U. Fantz, D. Reiter, B. Heger, D. Coster, J. Nucl. Mater. 290–293 (2001) 367.
[11] S. Kajita, S. Kado, S. Tanaka, Proceedings of the 10th International Symposium on Laser-Aided Plasma Diagnostics, 2001, 155.
[12] G.R. Mohelmann, F.J. De Heer, Chem. Phys. Lett. 43 (1976) 240.
[13] J.W. Wadehara, Appl. Phys. Lett. 35 (1979) 917.
[14] R.K. Janev, W.D. Langer, et al., Elementary Processes in Hydrogen–Helium Plasmas, Springer, 1987.
[15] O. Fukumasa, J. Phys. D 22 (1989) 1668.